# A New Species of Enyalius (Squamata, Leiosauridae) Endemic to the Brazilian Cerrado

Authors: M. Florencia Breitman, Fabricius M.C.B. Domingos, Justin C. Bagley, Helga C. Wiederhecker, Tayná B. Ferrari, et. al.

Source: Herpetologica, 74(4) : 355-369

Published By: Herpetologists' League

URL: https://doi.org/10.1655/0018-0831.355

*Herpetologica*, 74(4), 2018, 355–369


# A New Species of *Enyalius* (Squamata, Leiosauridae) Endemic to the Brazilian Cerrado

M. Florencia Breitman[1,6], Fabricius M.C.B. Domingos[1,2], Justin C. Bagley[1,3], Helga C. Wiederhecker[1,4], Tayná B. Ferrari[4], Vitor H.G.L. Cavalcante[1,5], André C. Pereira[1], Tarcísio L.S. Abreu[1], Anderson Kennedy Soares De-Lima[1], Carlos J.S. Morais[1], Ana C.H. del Prette[1], Izabella P.M.C. Silva[1], Rodrigo de Mello[4], Gabriela Carvalho[1], Thiago M. de Lima[4], Anandha A. Silva[1], Caroline Azevedo Matias[1], Gabriel C. Carvalho[1], João A.L. Pantoja[1], Isabella Monteiro Gomes[1], Ingrid Pinheiro Paschoaletto[1], Gabriela Ferreira Rodrigues[1], Ângela V.C. Talarico[4], André F. Barreto-Lima[1], and Guarino R. Colli[1]

[1] Departamento de Zoologia, Universidade de Brasília, Brasília, DF 70910-900, Brazil
[2] Instituto de Ciências Biológicas e da Saúde, Universidade Federal de Mato Grosso, Pontal do Araguaia, MT 78698-000, Brazil
[3] Departamento de Zoologia e Botânica, Universidade Estadual Paulista, São José do Rio Preto, SP 15054-000, Brazil
[4] Campus I, Universidade Católica de Brasília, Águas Claras, DF 71966-700, Brazil
[5] Instituto Federal do Piauí, Teresina, PI 64000-040, Brazil

Abstract: We describe a new species of *Enyalius* endemic to the Brazilian Cerrado, based on morphological and molecular data sets. In the face of uncertain taxonomy among museum specimens of *Enyalius*, we used a novel analytical approach based on Gaussian mixture modeling for species assignments. We also used a machine-learning classification procedure (random forests) to investigate morphological variation and identify species diagnostic characters. Phylogenetic and species delimitation analyses supported the distinction of the new species from its congeners. The new species is characterized by the fewest ventral scales and smallest snout–vent length in the genus. Moreover, we infer that this species diverged from its closest relative, *E. bilineatus*, in the late Miocene, presumably after colonization of Cerrado gallery forests by an Atlantic Forest ancestor, followed by ecological or geographical speciation linked to shrinkage or fragmentation of gallery forests associated with global cooling and increased aridity. Rapid conversion of natural habitats, the isolation of protected areas, and recent changes to the Brazilian Forest Code pose serious threats to the conservation of the new species described herein, and other gallery forest inhabitants.

**Key words:** Brazil; Conservation; DNA barcoding; Integrative taxonomy; Molecular data; Morphological data

The genus *Enyalius* (Wagler 1830) (Squamata, Leiosauridae) includes small- to medium-sized lizards restricted to Brazil (Etheridge 1969; Rodrigues et al. 2014) that are diurnal, ombrophilous, semiarboreal, and insectivorous (Vitt et al. 1996; Rautenberg and Laps 2010; Barreto-Lima and Sousa 2011; Maia-Carneiro et al. 2016). Coloration patterns are rarely exclusive to a given species, and are also highly variable within and between sexes (Jackson 1978). Ten species are currently recognized within *Enyalius* (Costa and Bérnils 2014): *E. brasiliensis*, *E. boulengeri*, *E. iheringii*, *E. perditus*, and *E. pictus*, mainly distributed in the Atlantic Forest; *E. erythroceneus* in the Caatinga; *E. leechii* restricted to the Amazon Forest; *E. catenatus* and *E. bibronii* in the Atlantic Forest and Caatinga; and *E. bilineatus*, mainly in the Atlantic Forest but also reported in the Cerrado. Recent molecular evidence indicates that other undescribed lineages might be present (Rodrigues et al. 2014).

The taxonomic history of *Enyalius* has been dynamic since its origins (Etheridge 1969; Jackson 1978). Over the last decade, the genus transitioned from having 6 recognized species (and 3 subspecies) to include 10 species. This change resulted from new species being described (Rodrigues et al. 2006), morphological evidence supporting the recognition of *E. catenatus*, *E. bibronii*, and *E. pictus* as full species, and molecular evidence supporting *E. brasiliensis* being reconsidered as a full species and the resurrection of *E. boulengeri* (Rodrigues et al. 2014). Phylogenetic relationships among *Enyalius* species were first proposed by Jackson (1978) using morphology, and later modified by Frost et al. (2001) based on a combination of morphological and mitochondrial DNA data. The first comprehensive molecular phylogeny of the genus was published only recently, however, based on one nuclear and three mitochondrial markers analyzed with the use of concatenation and species tree methods (Rodrigues et al. 2014).

Although *Enyalius bilineatus* is known to occur primarily in the Atlantic Forest, samples collected in the Cerrado have also been referred to this species (e.g., Rodrigues et al. 2014; Ledo and Colli 2016). Recent evidence indicates that these samples might represent an undescribed species. Rodrigues et al. (2014) inferred Cerrado samples as phylogenetically sister to *E. bilineatus*, with an estimated time of divergence from the most recent common ancestor ($t_{MRCA}$) around 6.86 million years ago (mya), in the late Miocene. Pairwise cytochrome-*b* genetic distances between *E. bilineatus* and its sister molecular lineage (including samples from Brasília, Distrito Federal and Mariana, Minas Gerais) are 14.5% (Vargas et al. 2015), which is a representative value among different lizard lineages (Breitman et al. 2012). Moreover, these two clades display marked differentiation, as they occur in different biomes without significant distributional overlap (Barreto-Lima 2012), their distributions are explained by unique combinations of bioclimatic predictors (Barreto-Lima 2012), and lizards from Brasília seem to be smaller than nominal *Enyalius* species, including samples of *E. bilineatus* from other areas.

Systematists have the responsibility to address the ongoing biodiversity crisis, which challenges us to publish accurate species descriptions (Wilson 1985; Wheeler 2004; Agnarsson and Kuntner 2007). Integrative taxonomy, in which several independent lines of evidence are used for species recognition (Dayrat 2005; Padial et al. 2010) under the

[6] Correspondence: e-mail, florbreitman@gmail.com

General Lineage Concept (species as independently evolving lineages; de Queiroz 2007), has become a useful framework to generate high-quality species descriptions (Pante et al. 2015). The goal of our study is to use molecular and morphological data to delimit and describe a new species of *Enyalius* lizard from the Cerrado in central Brazil. Given that downstream morphological, phylogenetic, and species delimitation analyses depend on the tip labels used (e.g., on guide trees; Yang and Rannala 2010; Yang 2015), we also develop a novel analytical framework to label samples objectively while dealing with uncertainty in taxonomic assignments and to identify traits robustly for species diagnosis.

## Materials and Methods

### Morphological Data

We studied 259 ethanol-preserved *Enyalius* samples collected from throughout Brazil (deposited in different museums), including representatives of all species and putative candidate species (Rodrigues et al. 2014; Fig. 1; also see the Supplemental Material 1 file, available online). We included samples from or near type localities (Table 1) of all species except for *E. brasiliensis*, as the only credible records of this species come from Rio de Janeiro (Rodrigues et al. 2014), ~1000 km north of the type locality in Santa Catarina (Lesson 1830). Rodrigues et al. (2014) recovered both *E. catenatus* and *E. perditus* as forming two polyphyletic and allopatrically distributed clades that diverged since the Miocene–Pliocene boundary (BEAST $t_{MRCA}$, *E. catenatus* = 14 mya; BEAST $t_{MRCA}$, *E. perditus* = 4.2 mya). *Enyalius catenatus* includes one clade distributed in Bahia (*E. catenatus* 1 in Rodrigues et al. 2014: Fig. 1) and another in Alagoas (*E. catenatus* 2). Given that the type locality of *E. catenatus* is Jequié, Bahia (Table 1), and assuming that samples collected at or near the type locality are more likely to belong to the nominal species, we considered the clade from Bahia as representing *E. catenatus* and the clade from Alagoas as an undescribed species. Similarly, *E. perditus* includes one clade from Juquitiba and Salesópolis, São Paulo (*E. perditus* 1 in Rodrigues et al. 2014: Fig. 1), and another from São Paulo and surrounding states (*E. perditus* 2). Given that *E. perditus* 1 includes samples from the type locality (Table 1), we assumed that it represents *E. perditus*, whereas "*E. perditus* 2" represents an undescribed species. We refer to populations from Brasília and surrounding areas (identified as *E. bilineatus* by Rodrigues et al. 2014) as *Enyalius* sp. and evaluate their specific status throughout the present study.

We assessed variation at 55 characters (24 meristic, 29 qualitative, and 2 morphometric characters; see Appendix and Supplemental Material 2, available online). We took measurements with rulers (±0.1 mm) and made scale counts and qualitative observations with stereomicroscopes. Scale counts and terminology followed Smith (1946), Etheridge (1969), Jackson (1978), and Rodrigues et al. (2006). Because of variation in character names among previous publications, however, we present a detailed list of character names and states (Appendix). Our study included several observers and, to minimize biases, we divided characters rather than samples among observers. Each observer collected data on one to a few characters, depending on their respective complexities (e.g., one observer was responsible only for collecting data on ventral scales). Because we could not unambiguously determine sex by checking cloacal or tail size and coloration patterns, we determined sex only when we unequivocally identified ovaries or testicles by dissection. We did not dissect individuals loaned from other collections, so our sample size for sexed individuals was limited in all species (except for *Enyalius* sp.). Because of these limitations, and following previous papers describing *Enyalius* species, we did not divide our data set by sex and compensated for this shortcoming by including multiple individuals per species from a range of sampling localities (see Jackson 1978; Rodrigues et al. 2006).

Table 1.—Type localities of *Enyalius* species according to original descriptions. All localities are in Brazil, and correct spellings or more precise definitions are given in parentheses.

| Species | Type locality |
|---|---|
| *E. bibronii* Boulenger 1885 | "Bahia" |
| *E. bilineatus* Duméril and Bibron 1837 | "Brésil" |
| *E. boulengeri* Etheridge 1969 | "Espirito Santo, Brazil" (=Espírito Santo) |
| *E. brasiliensis* (Lesson 1830) | "Sainte-Catherine du Brésil" (=Santa Catarina) |
| *E. catenatus* (Wied 1821) | "Cabeça do Boi" (=Jequié, Bahia; Bokermann 1957; Moraes 2009, 2011) |
| *E. erythroceneus* (Rodrigues et al. 2006) | "Fazenda Caraíbas, Mucugê, Bahia" |
| *E. iheringii* Boulenger 1885 | "Rio Grande do Sul" |
| *E. leechii* (Boulenger 1885) | "Santarem" (=Santarém, Pará) |
| *E. perditus* Jackson 1978 | "Estação Biológica de Boracéia, Município de Salesópolis, Estado de São Paulo, Brazil" |
| *E. pictus* (Schinz 1822) | "Mucurí, southeastern Bahía, Brazil" (=Mucuri, Bahia) |

After assembling an initial data set, we identified outliers for each trait and the corresponding observer remeasured specimens as needed, or noted if the measurement was a true outlier. We detected univariate outliers by using box plots and converting observations to Z-values, regarding those with $P(Z > |z|) < 0.0001$ as outliers. We also evaluated multivariate outliers by conducting a principal-components analysis of morphological characters, converting scores on the first two principal components to Z-values, and regarding those with $P(Z > |z|) < 0.0001$ as outliers.

### Taxonomic Assignment: Semisupervised Gaussian Mixture Modeling

When identifying specimens of *Enyalius*, researchers are often challenged by uncertainties resulting from uninformative original descriptions. To obtain an objectively labeled data set for downstream morphological and genetic analyses in the face of taxonomic uncertainty in the genus, we performed a semisupervised classification analysis (Weston et al. 2005). This analysis was based on Gaussian mixture models (GMM) with the bgmm R package (Biecek et al. 2012), as automated in GaussClust (Bagley 2017), and used all 55 morphological characters. In semisupervised classification, a subset of observations in a data set may be labeled (classified with certainty), while no information is provided about the labels (classes) of the remaining observations (e.g., because of dubious taxonomic IDs). The modeling approach then uses the knowledge of the labeled data to improve

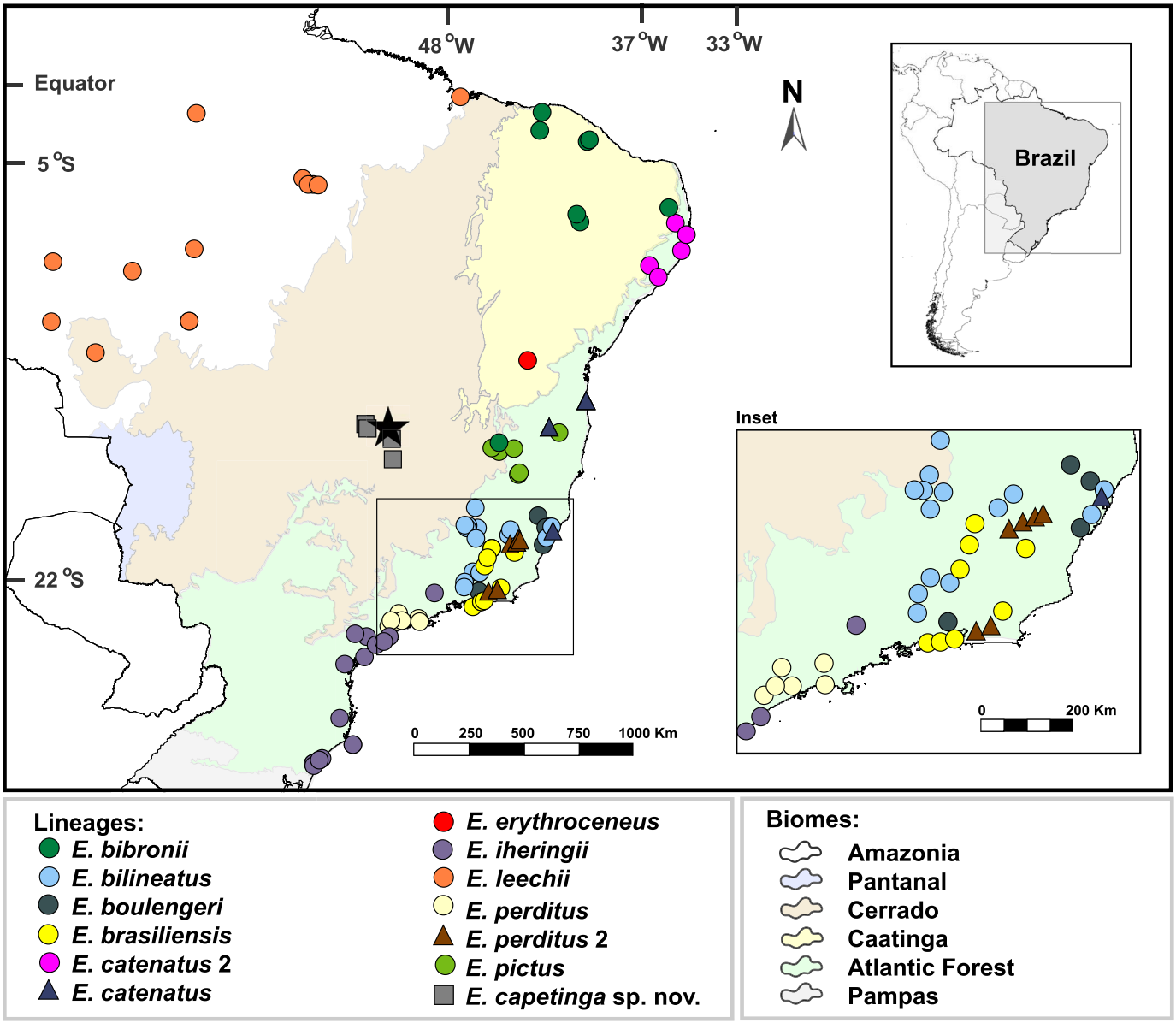


FIG. 1.—Distribution map of Brazilian biomes showing morphological sampling. The star indicates the type locality of *Enyalius capetinga* sp. nov. (Reserva Ecológica do IBGE, Brasília, Distrito Federal, Brazil; 15.9467°S, 47.8686°W; 1154 m above sea level). A color version of this figure is available online.

prediction of class membership (i.e., species assignment) of unlabeled observations. The goal of this analysis was not to perform a test of the validity of the described or undescribed species. Rather, this framework objectively labels, for downstream analyses, the individuals that could belong to described or undescribed taxa but (1) lacked appropriate diagnostic characters that could be matched to nominal species, (2) exhibited geographical overlap with other species (sympatry), or (3) lacked detailed locality data, or (4) lacked genetic data or were not from a locality for which genetic data were available for other individuals; (Supplemental Material 3, available online).

We started with a highly conservative and robust classification by providing unequivocal labels for 214 individuals (Set A) based on two sets of criteria. (1) For described species, we considered the simultaneous occurrence of ID labels from museum curators, proximity to type locality, and four easily distinguished morphological characters (EDMC) regarded as diagnostic (keeled vs. smooth subdigital lamella, keeled vs. smooth ventral scales, small vs. enlarged subocular scale, and presence vs. absence of dorsal crest; Etheridge 1969; Rodrigues et al. 2006). (2) For undescribed species, we compared the geographical sampling localities with the geographical distribution of the corresponding molecular lineage in Rodrigues et al. (2014), in addition to remoteness to known type localities, and variation at EDMC. Next, we subjected the unequivocally labeled specimens (Set A) along with the remaining, unlabeled specimens (Set B) to the semisupervised classification analysis with the use of bgmm (criteria presented in Supplemental Material 3). Unlabeled individuals that were then assigned to a species/lineage with high

probabilities by bgmm were double-checked and excluded from further analysis if a mistake could have been made, e.g., in cases of damaged specimens (Supplemental Material 4, available online). In downstream analyses, we only included the labeled specimens (Set A) plus a subset of the unlabeled individuals (Set B) that were subsequently classified with posterior probabilities >0.95 by our semi-supervised GMM, and met strict criteria used to decide whether or not a sample was known (Supplemental Materials 2, 4).

### Finding Morphological Differences: Guided Regularized Random Forest

After semisupervised GMM analyses, we arrived at a highly conservative and accurate data set including 228 individuals and 45 morphological characters (excluding "scales along the tail," which had a large amount of missing data, as well as monomorphic characters; see Appendix and Supplemental Material 2). We assessed morphological variation among species and identified the best predictors of species with the use of a guided regularized random forest (GRRF) analysis (Supplemental Material 5, available online). GRRF is an enhanced regularized random forest method where importance scores of a previous run on a complete training data set are used to guide the predictor selection process (Deng 2013). Importance scores are estimated by penalizing the selection of new predictors for splitting the decision tree when the gain (i.e., mean decrease in Gini impurity; Mingers 1989) is similar to that of features used in previous splits (Breiman 2001). Machine learning algorithms, such as support vector machines and GRRF, have been used in recent systematics papers (Murphy et al. 2016) and have been shown to outperform traditional linear methods (Domingos et al. 2014), while also avoiding their limitations (Quinn and Keough 2002). In addition, meristic data sets frequently do not meet linear model assumptions (Houle 1992); thus, applying linear classification methods to meristic data could lead to erroneous results (Cutler et al. 2007).

Prior to the GRRF analyses, we imputed 81 missing values (0.8% of the total data set) with the use of multivariate imputation by chained equation in the mice R package (van Buuren and Groothuis-Oudshoorn 2011), with 100 multiple imputations. To determine predictor importance in discriminating among *Enyalius* lineages/species, we implemented GRRF analyses in the RRF package (Deng 2013) on each imputed matrix, and calculated the average importance of each predictor across all runs. For each of the 100 imputed matrices, we also calculated GRRF model accuracy based on 50 replicates of fivefold cross-validation (Breiman and Spector 1992; Kohavi 1995), sequentially increasing the number of predictors based on their importance (Supplemental Material 5). Finally, to identify the best predictors of the new species, we conducted three GRRF analyses comparing the new species: (1) against *E. bilineatus* only (the closest relative of *Enyalius* sp.), (2) against all other species except *E. bilineatus*, and (3) against all species except *E. bilineatus* and *E. leechii* (*E. leechii* has a distinctively high number of vertebral scales). Analyses were performed in R v3.3.1 (R Core Team 2017).

### Molecular Data

We combined new and previously published genetic data (Supplemental Materials 6 and 7, available online) including 79 cytochrome-*b* sequences (cyt-*b*; 470 bp), 73 NADH dehydrogenase subunit four sequences (ND4; 817 bp), and 71 sequences of a nuclear protein-coding gene, the *c-mos* proto-oncogene (503 bp), for all described and candidate species. We selected these markers because they are phylogenetically informative for *Enyalius* (Rodrigues et al. 2014). Novel sequences included 14 individuals of *Enyalius* sp. from Brasília and surrounding areas, as well as 2 individuals of *E. bibronii* from Crato, Ceará. Remaining data from Rodrigues et al. (2014) were downloaded from GenBank. We treated samples identified as *E. bilineatus* in Rodrigues et al. (2014), but collected in Brasília, as *Enyalius* sp., and we treated samples identified as *E. catenatus* 1 and *E. perditus* 1 in Rodrigues et al. (2014: Fig. 1) as belonging to the nominal species. We used samples from specimens of *Anisolepis grillii*, *A. longicauda*, and *Urostrophus vautieri* (all Iguania:Leiosauridae) as outgroups.

We extracted genomic DNA with the use of Qiagen® DNeasy® 96 Tissue Kit, following the manufacturer's protocol. We amplified cyt-*b*, ND4, and *c-mos* with the primers and PCR protocols given in Rodrigues et al. (2014). We also sequenced a mitochondrial COI fragment (629 bp) for the holotype of the new species (CHUNB 74591) with the primers and PCR protocols described in Nagy et al. (2012). Sequencing was conducted on an ABI 3130*xl* sequencer and in-house protocols. We edited sequences with Geneious v9.1.7 (Kearse et al. 2012) and aligned them with PASTA v1.6.4 (Mirarab et al. 2015) with MAFFT used as the alignment algorithm, OPAL as merger, RAxML as the tree estimator (applying the GTR+G model), and an iteration limit setting of three. We assigned a barcode to the holotype of the new species and attached metadata to the sequence following the Barcode of Life Data System (BOLD) manual (Ratnasingham and Hebert 2007).

### Phylogenetic and Species Delimitation Analyses

Prior to phylogenetic analyses, we estimated a partitioning scheme with the use of PartitionFinder v2.1.1 (Lanfear et al. 2017), while separating all genes by codon position and estimating partitions under the GTR+G family of models. Models were selected based on the Akaike information criteria with the greedy algorithm (Lanfear et al. 2012, 2014). We ran maximum-likelihood phylogenetic analyses in RAxML v8.2.8 (Stamatakis 2014) with the use of partitions (Supplemental Material 8, available online), and estimated nodal support with 100 rapid bootstraps. We considered nodal support significant or moderate for bootstrap values over 95% (Felsenstein and Kishino 1993) and 70% (Hillis and Bull 1993), respectively. Bayesian inference analysis was performed in ExaBayes v1.5 (Aberer et al. 2014) with the same partition schemes and linking branch lengths across partitions. We performed two independent runs with four chains each, starting from a parsimony tree, for at least one million generations (sampling every 500th) until the average standard deviation of split frequencies was below 0.01, indicating good convergence. A minimum acceptable effective sample size of 200 was reached for all parameters, and we checked the potential scale reduction factor (~1.0)

with the use of the postProcParam and extractBips utilities distributed with ExaBayes. We considered Bayesian posterior probabilities >0.95 as significant (Huelsenbeck and Ronquist 2001). All of the above phylogenetic analyses used tip labels (individually or in aggregate) derived from the semisupervised GMM analyses in bgmm.

We tested species limits among *Enyalius* by conducting joint Bayesian species delimitation and species tree estimation in BPP v3.3 (Yang 2015). This program uses the multispecies coalescent model and accounts for incomplete lineage sorting attributable to ancestral polymorphism and gene tree-species tree conflict (Yang and Rannala 2010, 2014). Individuals were assigned to species hypotheses (putative new and nominal species) based on their placement in the Bayesian and ML phylogenetic trees, and on results from the semisupervised GMM analysis. We ran BPP for $5 \times 10^5$ generations, sampling every 5 generations, and discarding the first 10,000 steps as burn-in. To account for potentially different speciation histories, we ran BPP with different gamma priors on population sizes ($\theta$s) and age of the root of the species tree ($\tau_0$), as follows: (1) large population size and deep divergence, ~G(2, 1000) for both priors; (2) small population size and shallow divergence, ~G(1, 10) for both priors; (3) large population size and shallow divergence, ~G(2, 2000) for $\theta$s, ~G(1, 10) for $\tau$s; (4) small population size and deep divergence, ~G(1, 10) for $\theta$s, ~G(2, 2000) $\tau$s; and (5) intermediate values of ~G(2, 100) for both priors. Other divergence time parameters were assigned a Dirichlet prior (Yang and Rannala 2010: Equation 2). We also used both available cleandata options (one using the data as is, and the other omitting gaps or ambiguity characters). We checked for convergence by running BPP twice for each prior and cleandata option, starting from different random trees. All runs returned very similar results; thus, we report results from eight runs (four for each cleandata option) with ~G(2, 1000) used for both priors, which represent realistic biological choices for the species (Sturaro and da Silva 2010; Barreto-Lima and Sousa 2011; Rodrigues et al. 2014).

## RESULTS

### Morphological Results

The classification derived from semisupervised GMM analysis assigned 17 of the unlabeled individuals (unknowns) to a species with high posterior probability ($P > 0.95$) and, in seven cases, the assignment matched their original field/curator IDs (Supplemental Materials 3–5). We identified 3 individuals, of the 17 unknowns classified with high posterior probability, as potentially being erroneously classified (see Supplemental Materials 3–5). The remaining 14 individuals were labeled according to the bgmm results. Our final matrix included 45 morphological characters measured for 228 individuals of *Enyalius* (Appendix and Supplemental Materials 2–5). Means ± 1 SD, and ranges, for predictors and lineages are presented in Supplemental Material 2.

Across lineages, the GRRF results (Fig. 2) revealed a cross-validation error ranging from 0.65–0.1 (corresponding to using the single best predictor to using all predictors). The GRRF model based on the five best predictors (ventrals, vertebrals, suboculars, scales around the tail, and paravertebrals) had an accuracy of ~70%, based on 5000 replicates of fivefold cross-validation (Fig. 2). The GRRF model comparing the new species with pooled samples of all other species except *E. bilineatus* identified ventrals, supraciliaries, paravertebrals, gulars (from mental scale to gular fold), and suboculars as the best predictors. Likewise, the model comparing the new species against *E. bilineatus* identified the number of ventral scales, shape of lateral scales, number of dorsolateral tibials, and tail length as the four best predictors (details in Supplemental Material 9, available online). Overall, our GRRF results highlight several dimensions of morphological evidence supporting *Enyalius* sp. as a new species. Preliminary GRRF analysis also indicated that *E. catenatus* 2 and *E. perditus* 2 are morphologically different from other *Enyalius* species (*E. catenatus* 2: number of dorsolateral tibials, number of vertebral and midbody scales; *E. perditus* 2: number of ventral, paravertebral, and midbody scales).

### Phylogenetic Analyses and Species Delimitation Results

Our maximum-likelihood and Bayesian inference reconstructions showed congruent results (Fig. 3; Supplemental Material 10, available online). We recovered individuals from each nominal and putative new species in distinct clades with significant to moderate nodal support, and with an overall similar topology (cf. Rodrigues et al. 2014). Minor differences between the Bayesian and ML trees were only observed in the placement of individuals within species. Our species delimitation analyses inferred nominal and putative new *Enyalius* species as different entities with posterior probabilities above 0.93 in cleandata runs, and above 0.99 in no cleandata runs. No other species hypothesis had a posterior probability of more than 0.05, and the hypothesis of 16 full species (including outgroups) had the highest posterior probability across runs. Finally, the coalescent species tree estimated by BPP recovered *E. leechii* and *E. erythroceneus* in a different position compared to ML and Bayesian concatenated estimations (Supplemental Material 10). These differences had no influence on the species delimitation results, but they should be addressed in future research that incorporates additional molecular markers and broader geographical sampling. Overall, we found strong molecular support for *Enyalius* sp. being a new species, because BPP inferred the corresponding samples as forming a distinct species with posterior probability of 1 in all runs. This species was also strongly supported as sister to *E. bilineatus* across the BPP coalescent species tree, as well as Bayesian and maximum- likelihood gene trees.

## SPECIES DESCRIPTION

*Enyalius* ***capetinga*** sp. nov.
(Figs. 4–6)

*Enyalius bilineatus*: Rodrigues et al. (2006: 11–24), Rodrigues et al. (2014: 137–146), Ledo and Colli (2016: 98–109).

*Enyalius* aff. *bilineatus*: Nogueira et al. (2009: 83–96).

**Holotype.**—CHUNB 74591 (Figs. 4, 5), an adult male collected by Ana Cecília Holler Del Prette and Anderson Kennedy Soares de Lima on 10 June 2016 at Reserva Ecológica do IBGE (Instituto Brasileiro de Geografia e Estatística, Fig. 7), Brasília, Distrito Federal, Brazil

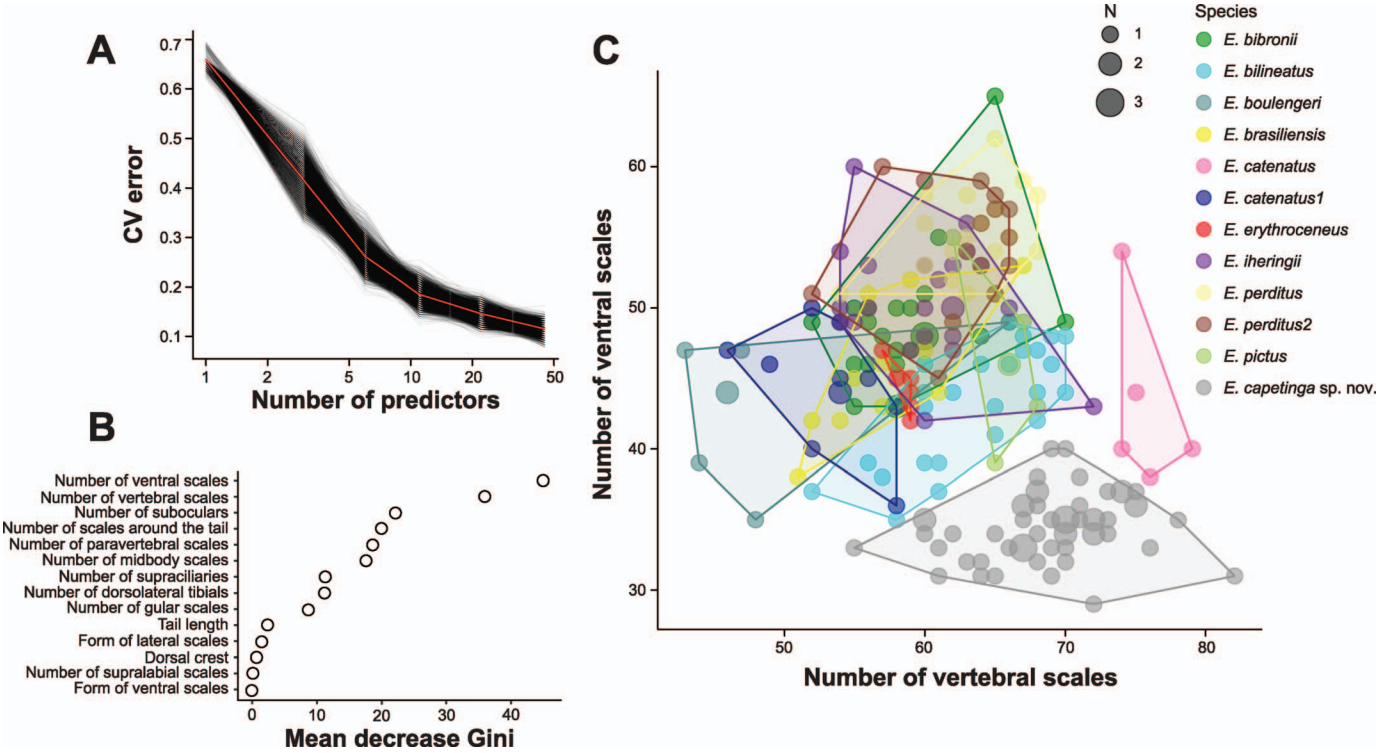


FIG. 2.—Guided regularized random forest (GRRF) results for *Enyalius* morphological data. (A) Prediction error of GRRF models based on increasing number of predictors ranked by importance, based on 50 replicates of fivefold cross-validation for each of 100 multiply imputed data sets. (B) Importance of morphological predictors in correctly assigning individual lizards to species of *Enyalius* based on mean decrease in Gini accuracy of GRRF models, based on 50 replicates of fivefold cross-validation for each of 100 multiply imputed data sets. The higher the mean decrease in Gini accuracy, the higher the predictor importance. Only the 10 most important predictors are presented. (C) Variation in number of ventral and vertebral scales, the two best predictors of differences among species/lineages of *Enyalius* (to improve visualization, *E. leechii* is not included in the plot because it is highly distinct from other lineages).

(15.9467°S, 47.8686°W; 1154 m above sea level [asl]; in all cases, datum = WGS84).

**Paratypes.**—CHUNB 8173, 8906, 29290, 29292, and 29295 adult males, 23847 juvenile male, and CHUNB 8168, 8182, 29312, 52396, 52407 adult females; all from Brasília, Distrito Federal, Brazil (14.7572 S, 47.9761 W [1154 m asl] except for CHUNB 52497 from 15.9467 S, 47.8686 W [1154 m asl]); collected by Guarino Rinaldi Colli and students of Universidade de Brasília, except for CHUNB 52407 collected by Roger Maia Dias Ledo. Paratypes collected between 1994 and 2008. Specifically, CHUNB 8173 on 9 May 1994, CHUNB 8906 between 1994 and 1998, CHUNB 29290, 29292, 29295, and 29312 between 2001 and 2003, CHUNB 23847 in 2001, CHUNB 8168 on 15 June 1994, CHUNB 8182 on 22 August 1991, CHUNB 52396 on 23 April 2008, and CHUNB 52407 on 20 May 2008.

**Diagnosis.**—*Enyalius capetinga* differs from *E. bilineatus* mainly in having fewer ventral (34.45 ± 2.25 [29–40] vs. 43.2 ± 4.06 [35–49] in *E. bilineatus*) and dorsolateral tibial scales (10.38 ± 1.29 [8–13] vs. 12.52 ± 0.59 [12–14] in *E. bilineatus*), and a higher number of midbody (52.96 ± 4.34 [42–64] vs. 45.8 ± 3.64 [39–52] in *E. bilineatus*) and vertebral scales (68.8 ± 4.94 [55–82] vs. 63.56 ± 4.88 [52–70] in *E. bilineatus*; Table 2; Supplemental Materials 2 and 10). Also, all samples of *E. capetinga* present granular lateral scales, whereas only 32% of *E. bilineatus* samples present this character state, and the remaining individuals (68%) present non-granular scales. *Enyalius capetinga* differs from all other species of the genus (excluding *E. bilineatus*; see character summary in Table 2 and Supplemental Materials 2, 10) mainly in having the smallest count of ventral scales (34.45 ± 2.25), supraciliaries (6.59 ± 1.64), paravertebral scales (63.84 ± 5.96), dorsolateral tibials (10.38 ± 1.29), supralabials (7.86 ± 1.03), and scales from mental to gular fold (34.34 ± 4.04). Likewise, the new species is distinguished from all others in the genus by having keels on most dorsal scales. *Enyalius capetinga* differs from most other *Enyalius* species in lacking contact between nasal and postrostral scales (absent in 89% of the samples), which is common in most other species (excluding *E. bilineatus* and *E. pictus*); having an enlarged subocular scale (present in 96% of *E. capetinga* samples) that is smaller in the majority (>70%) of individuals of other species (except *E. bilineatus*, *E. pictus*, and *E. erythroceneus*). *Enyalius capetinga* differs from *E. leechii* in having a dorsal crest and smooth fourth toe lamellae, from *E. bibronii* in having keeled ventral scales, and from *E. boulengeri* and *E. brasiliensis* in having smooth infracarpals (Supplemental Material 2).

**Description of holotype.**—Adult male; snout–vent length (SVL) 68 mm; tail length (complete, not regenerated) 185 mm; axilla–groin distance 30.1 mm. Distance between anterior edge of the auditory meatus and posterior edge of eye 6.8 mm; external auditory meatus conspicuous, higher (2.2 mm) than wide (1.6 mm). Head 15.7 mm in length (from anterior border of auditory meatus to center of rostral scale),

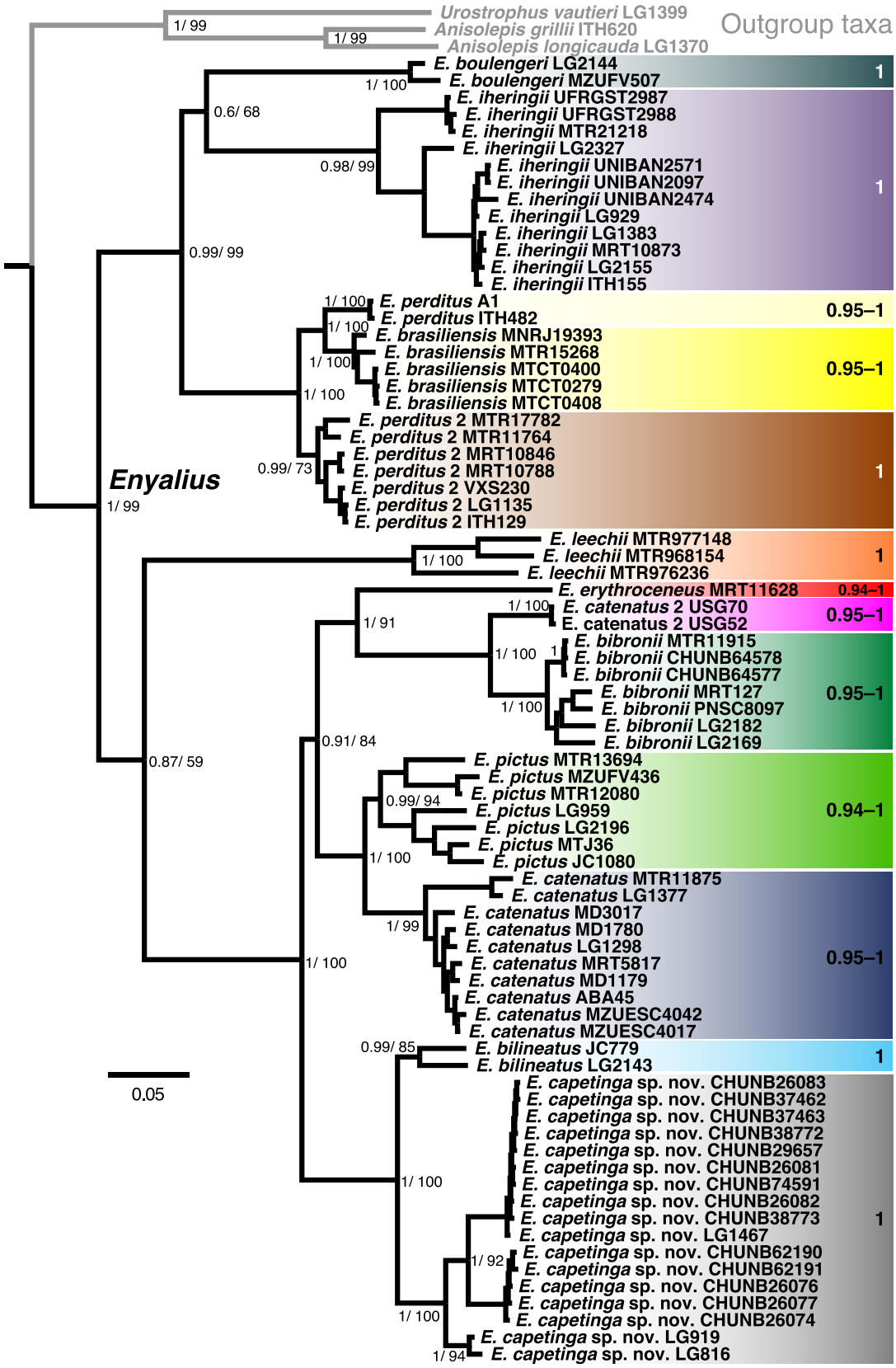


FIG. 3.—Phylogenetic relationships among *Enyalius* species as estimated by Bayesian inference and maximum-likelihood analyses. Posterior speciation probabilities estimated in BPP for each species/lineage are given at right. Numbers along nodes denote posterior probabilities for the Bayesian analysis and bootstrap scores from the maximum-likelihood analysis. A color version of this figure is available online. Scale indicates rate of base substitutions per site.

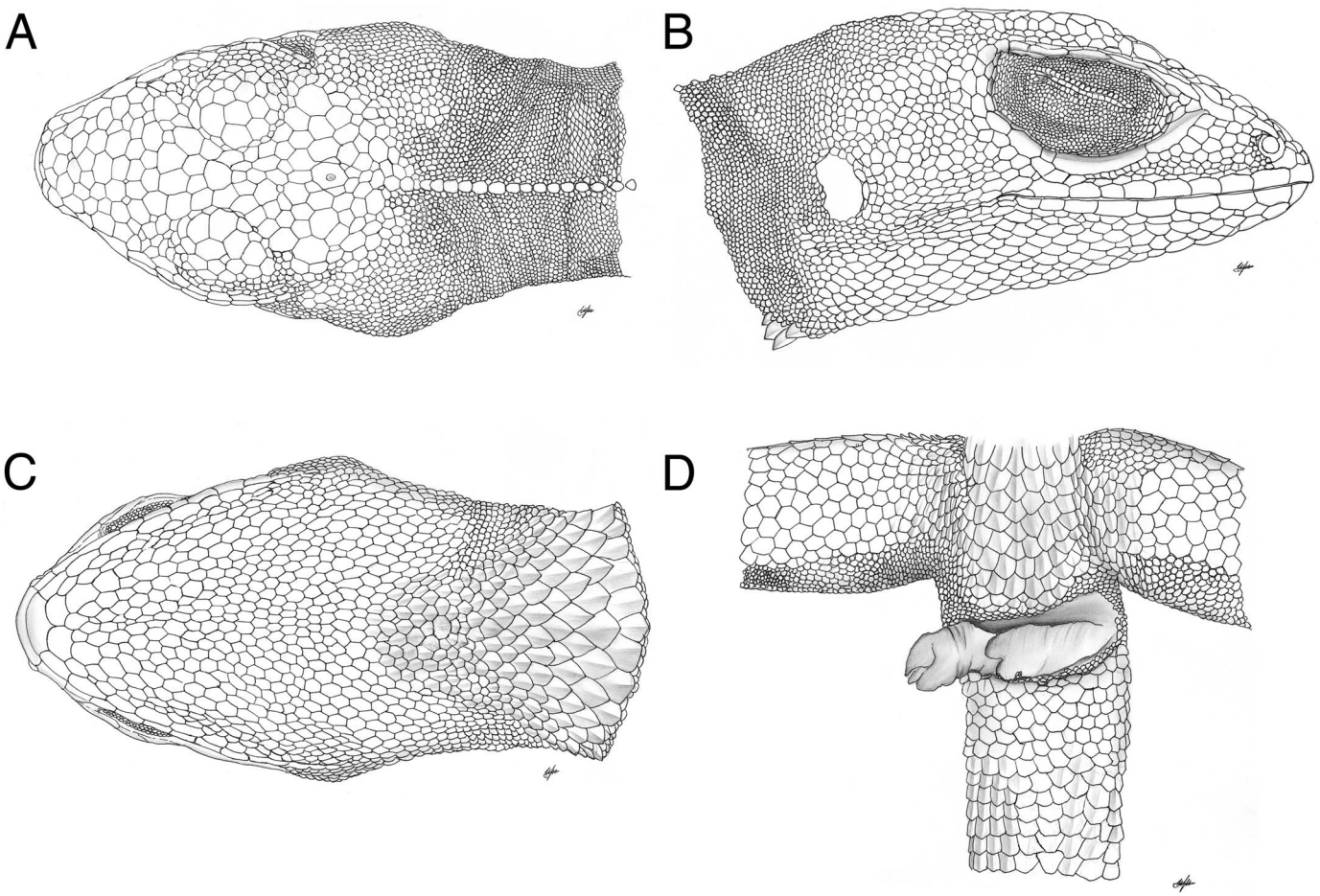


FIG. 4.—Squamation of the *Enyalius capetinga* holotype (CHUNB 74591, adult male): (A) dorsal view of head, (B) lateral view of head, (C) ventral view of head, and (D) cloacal region.

11.8 mm wide (at temporal region), and 9.8 mm high (at parietal region). Snout length 7.4 mm (from posterior corner of eye to center of rostral scale). Eye length 4.1 mm; eye (from anterior edge) to nostril distance 5.6 mm. Forelimb length 19.1 mm (excluding hand); hindlimb length 30 mm (excluding foot); hand length 15.1 mm (wrist to tip of fourth finger excluding claw); foot length 29.9 mm (ankle to tip of fourth toe excluding claw).

FIG. 5.—Photograph of the *Enyalius capetinga* holotype (CHUNB 74591, adult male). Inset shows ventral aspect of specimen (photo credits: M.F. Breitman and C.J.S. Morais). A color version of this figure is available online.

Dorsal head scales irregular in size and shape (quadrangular or rhomboidal), juxtaposed, smooth, decreasing in size and becoming granular in the temporal region and towards the body. Rostral rectangular, wider (3.2 mm) than high (1.0 mm), contacting six postrostrals that separate nasal from rostral. Nasals rounded, surrounded by 10–11 scales; nostril occupies most of nasal, laterally oriented. Six quadrangular internasals. Nineteen scales between rostral and occipital scales. Interparietal smooth and rounded, surrounded by eight smaller scales; pineal eye in the center of the scale but not very evident. Parietals similar in size to interparietal, slightly bulged and irregularly shaped. Circumorbital semicircles (10–11 scales) defined by smaller smooth scales, separated by one big scale at the closest point. Supraoculars in 6–7 rows, quadrangular, similar in size to frontal, becoming smaller towards the superciliary ridge. Canthal ridge straight, with one rounded and one enlarged scale (quadrangular, bulged) that connects the superciliaries with the nasal scale.

Loreals in 6–7 series, juxtaposed, smooth or slightly bulged, mostly quadrangular. Loreals variable in size; smaller ones (half the size of large ones) near the nasal and supralabial areas. Eight elongated and juxtaposed superciliaries; the three anterior ones much more elongated

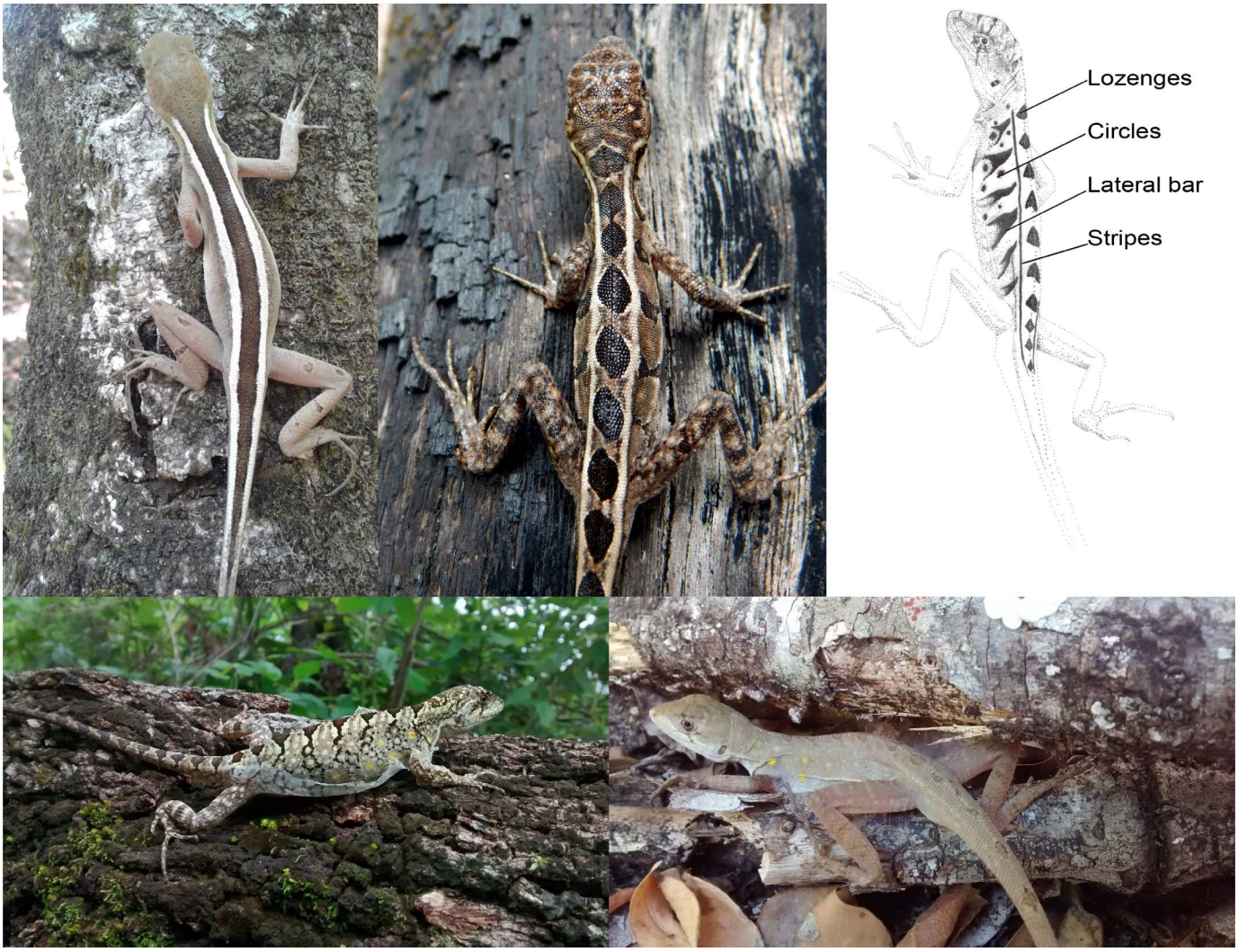


FIG. 6.—Pattern polymorphism in *Enyalius capetinga* sp. nov. Drawing in upper-right panel shows the four components of dorsal coloration patterns observed (illustration credit: Mariana G. Zatz).

(2.2 mm) than the posterior ones (0.7 mm). Preocular and subocular enlarged (2.3 and 3.3 mm, respectively), longer than wide (0.7 mm), keeled along their upper border. Eight smaller quadrangular postoculars. Ocular region covered with granular scales, except for quadrangular, juxtaposed palpebrals. Nine supralabial scales, separated from subocular by one row of juxtaposed scales. Temporals larger than granular occipitals, juxtaposed, quadrangular, somewhat bulged. Nine and eight infralabials on the right and left sides of holotype, respectively. Lateral gulars juxtaposed, slightly smaller than ventral gulars. Anterior auriculars similar to adjacent posterior temporals; posterior auriculars smaller, granular, and similar to scales on sides of neck. External auditory meatus conspicuous, higher (2.4 mm) than wide (1.4 mm).

Mental small, pentagonal, wider (2.2 mm) than high (1 mm). Thirty-seven gulars between mental and collar (1–27 gradually shift from rounded to slightly keeled; remaining scales mucronated and imbricated). First row of postmentals with two scales, followed by row of six scales; postmentals juxtaposed, elliptical, slightly bulged until transforming into gulars. Gulars slightly imbricated, keeled and mucronated, similar in shape to ventrals but slightly larger towards collar fold. Smaller granular scales hidden between pledges of gular fold with very small granules filling the space among them. Collar continues dorsolaterally, forming a prehumeral fold.

Dorsal crest formed by 77 enlarged vertebral scales ($\sim$1 $\times$ 0.7 mm), pyramidal in the occipital region (scales 1–24) and becoming keeled, mucronated, elongated, and slightly imbricated at the forelimb level until the hindlimbs (scales 25–50), where they became quadrangular and slightly keeled from there to the first 1/10th (17 mm) of the tail length. Nuchal and lateral scales small ($<$0.2 mm), granular. Paravertebral scales (counted three rows right of middorsum), slightly imbricated, quadrangular ($\sim$0.5 $\times$ 0.5 mm), somewhat keeled; 125 paravertebral scales between occiput and anterior insertion of hindlimb; 75 paravertebral scales between posterior insertion of forelimb and anterior insertion of hindlimb. Thirty-seven rows of ventrals (from posterior insertion of forelimb to anterior insertion of hindlimb; 53 rows from gular fold to cloaca) at least four times larger (1.2 $\times$ 1.3 mm) than dorsals, flat, keeled, slightly mucronated but rounded. One hundred six scales around


FIG. 7.—Satellite view of the type locality for *Enyalius capetinga* sp. nov. (dotted pin symbol), within a gallery forest of the Cerrado biome. A color version of this figure is available on line.

midbody. Hemipenis mostly everted; no distinguishable femoral or preanal pores.

Suprabrachials and antebrachials larger than dorsal and crest scales, imbricated, rhomboidal, keeled, becoming granular near the axilla. Infrabrachial scales small, granular. Supracarpals strongly imbricated, rhomboidal, keeled, slightly mucronated. Infracarpals imbricate, elongated, rounded. Lamellae of the hands quadrangular, strongly imbricated, nonmucronated, not keeled. Infradigital lamellae of the left hand in each finger (in parentheses: counts for the right hand when different from left hand): I:8, II:12, III:18 (20), IV:19 (missing finger), V:12. Claws robust, curved, sharp, light brown. Suprafemorals larger than dorsal and crest scales, rhomboidal, imbricated, varying in size and shape, small and smooth near the body and the infrafemorals, bigger and keeled toward the knee. Infrafemorals small, granular. Tibials rhomboidal, imbricated, keeled, slightly mucronated, smaller and granular toward the foot. Supratarsals strongly imbricated, rhomboidal, keeled, slightly mucronated. Infratarsals juxtaposed, rounded. Lamellae of the feet quadrangular, strongly imbricated, nonmucronated, not keeled. Infradigital lamellae of the left feet in each finger (in parentheses: counts for the right feet when different from left): I:8 (missing), II:12 (13), III:20 (18), IV:26—missing a section (30), V:15 (missing). Claws robust, curved, sharp, light brown.

Tail complete, nonregenerated, 2.72 times longer than SVL. Dorsal and lateral caudal scales keeled, smaller, juxtaposed in anterior portion of tail, increasing in size and becoming imbricated towards tail tip. Ventral caudal scales keeled and mucronated, like caudal posterior scales.

**Variation.**—In *Enyalius capetinga*, we found sexual dimorphism in tail length (females = 170.40 ± 30.31 mm, 120–211 mm; males = 183.45 ± 18.03 mm, 154–221 mm), SVL (females = 71.33 ± 9.03 mm, 55–88 mm; males = 68.76 ± 5.27 mm, 61–80 mm), and the ratio of tail length to SVL (females = 2.39 ± 0.33, 1.51–2.92; males = 2.67 ± 0.15, 2.31–3.00). No other characters presented statistically significant sexual dimorphism (Supplemental Material 2). With the use of >200 lizards collected in and around Brasília, Zatz (2002) identified four components of coloration patterns in *E. capetinga*: (1) dorsal lozenges along vertebral line (reaching tip of tail; present in 86.5% of individuals); (2) yellow lateral circles (varying in size and number; 73.4%); (3) lateral bars (complete or punctuated, perpendicular to body axis, between paravertebral and ventral region; 45.7%); and (4) white paravertebral stripes (35.2%; Fig. 6). The more common coloration combinations were: lozenges + circles (34.1%), followed by lozenges + bars + circles (24.7%; as in the holotype), and lozenges + stripes + bars (14.2%). Although no exclusive patterns were associated with sex, the patterns of lozenges + bars + stripes and stripes were found in females more than twice as often as in males; and the patterns lozenges + bars + circles, lozenges + circles, lozenges + stripes, and circles were more than twice as common in males than in females. Coloration patterns are not associated with sexual maturity, climate seasonality, or sex. Immature individuals are statistically more likely to present lateral bars than mature individuals. Tail coloration presents lozenges and perpendicular bars in all individuals (Zatz 2002).

TABLE 2.—Values of the most informative diagnostic characters among species of *Enyalius*. Values for meristic variables are presented as means ± 1 SD followed by range in parentheses. The character "Dorsal scales shape" is qualitative and values are presented as a ratio of frequencies, with relative frequencies listed in parentheses after absolute frequencies. Ranges of samples sizes are listed in parentheses after species names. Studied variables, data, and summary statistics of all variables are presented in the Appendix and in Supplemental Material 2.

| | Ventral scales | Supraciliaries | Paravertebral scales | Gular scales | Supralabials | Dorsolateral tibials | Dorsal scales shape[a] |
|---|---|---|---|---|---|---|---|
| *E. bibronii* (22–23) | 48.64 ± 4.6 (43–65) | 10.09 ± 0.95 (8–12) | 83.14 ± 6.68 (73–98) | 39.04 ± 4.17 (32–49) | 10.43 ± 0.79 (9–12) | 12.35 ± 1.07 (10–15) | 4 (0.17):13 (0.57):6 (0.26) |
| *E. bilineatus* (25) | 43.2 ± 4.06 (35–49) | 7.48 ± 2.31 (5–16) | 62.04 ± 6.82 (51–73) | 36.76 ± 3.99 (29–44) | 7.68 ± 0.85 (6–9) | 12.52 ± 0.59 (12–14) | 0:0:25 (1) |
| *E. boulengeri* (7) | 43.57 ± 4.96 (35–49) | 11 ± 1.53 (10–14) | 89.14 ± 10.92 (75–108) | 50.14 ± 3.58 (44–56) | 10.29 ± 0.76 (9–11) | 12.43 ± 1.27 (11–15) | 0:7 (1):0 |
| *E. brasiliensis* (10–11) | 45.1 ± 4.43 (38–53) | 10.6 ± 0.84 (9–12) | 90.18 ± 7.59 (75–98) | 50.18 ± 3.43 (46–56) | 10.09 ± 0.7 (9–11) | 13.64 ± 1.29 (12–16) | 0:11 (1):0 |
| *E. catenatus* 2 (5) | 43.2 ± 6.42 (38–54) | 9.2 ± 1.79 (8–12) | 87.6 ± 3.21 (83–91) | 41.8 ± 3.7 (39–48) | 10.4 ± 1.52 (8–12) | 15.6 ± 2.51 (14–20) | 0:5 (1):0 |
| *E. catenatus* (11) | 44.45 ± 3.93 (36–50) | 11.64 ± 1.03 (10–13) | 88.27 ± 7.67 (78–102) | 46.64 ± 4.03 (42–55) | 11.18 ± 1.6 (8–14) | 17.18 ± 2.6 (14–20) | 0:11 (1):0 |
| *E. erythroceneus* (6) | 44.33 ± 1.75 (42–47) | 8.67 ± 1.51 (7–11) | 79.17 ± 3.82 (75–84) | 38.33 ± 3.33 (33–42) | 9.5 ± 1.22 (8–11) | 11.67 ± 1.37 (10–13) | 0:6 (1):0 |
| *E. iheringii* (22–23) | 50.23 ± 3.85 (42–60) | 13.7 ± 1.99 (10–17) | 75.3 ± 8.34 (59–102) | 44.09 ± 2.66 (39–49) | 11.09 ± 1.12 (8–13) | 13.04 ± 1.22 (11–15) | 7 (0.3):11 (0.48):5 (0.22) |
| *E. leechii* (22) | 39.45 ± 2.7 (35–44) | 11.23 ± 1.31 (8–13) | 84.73 ± 5.74 (74–94) | 55.05 ± 5.13 (47–67) | 11.18 ± 0.73 (10–12) | 17 ± 3.31 (12–22) | 0:17 (0.77):5 (0.23) |
| *E. perditus* (18) | 55.22 ± 3.08 (51–62) | 10.33 ± 1.14 (8–12) | 101 ± 6.18 (90–114) | 51.44 ± 3.33 (46–58) | 9.67 ± 1.08 (8–12) | 13 ± 1.5 (11–18) | 0:18 (1):0 |
| *E. perditus* 2 (15) | 54.47 ± 4.21 (45–60) | 10.4 ± 1.18 (8–12) | 93.73 ± 12.19 (72–114) | 48.6 ± 4.22 (43–56) | 9.6 ± 1.12 (9–13) | 12.73 ± 1.03 (12–15) | 0:14 (0.93):1 (0.07) |
| *E. pictus* (6) | 46.33 ± 5.43 (39–55) | 10.33 ± 1.37 (8–12) | 92.17 ± 3.97 (85–97) | 46.5 ± 3.94 (40–52) | 11.33 ± 1.03 (10–13) | 18.17 ± 3.6 (13–23) | 0:5 (0.83):1 (0.17) |
| *E. capetinga* (56) | 34.45 ± 2.25 (29–40) | 6.59 ± 1.64 (4–14) | 63.84 ± 5.96 (51–77) | 34.34 ± 4.04 (28–47) | 7.86 ± 1.03 (6–12) | 10.38 ± 1.29 (8–13) | 0:2 (0.04):54 (0.96) |

[a] States of the characters are listed in the following order: mostly smooth, mostly granular, and mostly keeled.

**Coloration of holotype in life.**—Dorsal background gray; ventral background white (Fig. 5). Dorsum of head brownish (relative to the laterals and rest of body), with black, thin, uneven, transversal lines; small scattered dark spots on remaining gray scales. Two anterior lines between rostral and superciliaries, less defined and thinner than three posterior ones that reach superciliaries. Temporal region with smaller black line. Sides of head change gradually from dorsal coloration to ventral coloration. Two black lines (like posterior lines of dorsal head) between eye and last supralabial and anterior auricular scales. Suboculars with black spots. Ventral head coloration white, with some scattered black spots.

Coloration of temporal area like anterior region; black, thin, uneven lines form V-like shape that transitions into larger, darker, thicker lines (almost twice as large as lines on head), surrounded by white scales defining eight transversal lozenges along the body. Dorsolateral parts of body (between neck and forelimbs) gray, with several pairs of thinner punctuated lines continuing, at the uppermost end, to the dorsal lozenges and fading away at the bottom, where coloration shifts to ventral white. Sides of body with 8–9 conspicuous, bright, yellow, large (each including 6–30 scales) spots, concentrated in the anterior region, and several white/yellowish smaller (1–2 scales) spots in remaining area. Venter white, almost immaculate, with black spots on a few scales.

Tail dorsally gray, with diamondlike black blotches that along the first third of the tail transforming into grayish marks that dissolve into a gray/brownish tail. Limbs dorsally variegated, gray, with some black marks that form lines. Ventrally, limbs and tail white with some grayish spots.

**Coloration of holotype in preservative.**—After 6 mo in preservative, coloration turns dark gray (darker than in life). Even though all brownish and yellow colors turn gray, dorsal lozenges on the body, limbs, and tail remain noticeable. Dorsolateral coloration homogeneously gray with black lines; yellow and white spots faded and undistinguishable. Venter white; ventral parts of limbs and tail darker gray/brownish.

**Etymology.**—The specific epithet of this species is a Portuguese word that refers to Capetinga Creek, located in Fazenda Água Limpa, property of Universidade de Brasília, ~7 km SW of the type locality, where GRC collected the first specimens of *Enyalius capetinga* in November 1987. Capetinga is formed by the combination of the Tupinambá language (Tupi-Guarani) words "kapi'" (grass) and "tinga" (dry/white), meaning "dry grass." We also chose this name for the resemblance with "capeta," a Portuguese word for "devil" or "bugbear." Sometimes, while conducting our investigation and dealing with the complex interactions of academic life, we felt as if the *capeta* was coming to get us!

**Distribution.**—*Enyalius capetinga* is endemic to the Brazilian Cerrado, and is known from Brasília, Distrito Federal and nearby localities in Minas Gerais (Paracatu and Unaí; Fig. 1).

**Barcoding of holotype.**—BOLD records (sequence and specimen metadata) can be accessed at http://www.boldsystems.org/index.php/Public_RecordView?processid=CHUNB001-17.

**Natural history.**—*Enyalius capetinga* inhabits primarily gallery forests, but some individuals were collected in nearby areas of cerrado sensu stricto and cerradão. Cerrado sensu

stricto is the most common vegetation physiognomy of Cerrado, characterized by the dominance of trees and shrubs, 3–8 m tall, with more than 30% of canopy cover, with a fair amount of herbaceous vegetation among them. The cerradão is denser, with 30–90% of canopy cover, dominated by 8–12 m tall trees and very reduced herbaceous vegetation (Oliveira-Filho and Ratter 2002). The new species is diurnal, oviparous, ombrophilous, and feeds primarily on arthropods (Zatz 2002). Females reach sexual maturity at a larger size than males (females = 71 mm SVL, males = 57.82 mm SVL) and breeding occurs from September to February (Zatz 2002). The distributional range of the new species is characterized by the Aw climate in Köppen's classification, with marked rainfall seasonality: a dry, cold season from May to September, and a wet, hot season from October to April (Alvares et al. 2013). The annual mean temperature in Brasília is 20.6°C (16.1–26.6°C) and the annual mean precipitation is 1540.6 mm, of which 1413 mm (91.7%) occurs in the wet season (Ramos et al. 2009).

## Discussion

Accurate species descriptions are necessary when addressing the ongoing biodiversity crisis, and for supporting other disciplines that rely on accurate taxonomy (Wilson 1985; Wheeler 2004; Drew 2011). We set out to test the hypothesis that populations of *Enyalius* lizards from central Brazil identified by previous molecular and ecological studies (Barreto-Lima 2012; Rodrigues et al. 2014; Vargas et al. 2015) constituted a new species, by generating and analyzing morphological data (100% novel; 55 variables for 259 individuals) and molecular data (~20% novel; three genes for ~75 individuals) for the genus. Our approach—combining semisupervised Gaussian mixture modeling followed by machine-learning classification—required a greater investment of time than alpha taxonomy methods, but minimized the problem of overconfidence in museum identifications and produced more detailed species hypotheses (Sangster and Luksenburg 2015). Our species delimitation results supported the recognition of *E. brasiliensis* and *E. boulengeri*, establishing that *E. perditus* 2 and *E. catenatus* 2 (sensu Rodrigues et al. 2014), and *E. capetinga* are independently evolving lineages. Although GRRF analysis indicated that samples of *E. catenatus* 2 and *E. perditus* 2 were also morphologically different from other congeners; these species await formal description.

*Enyalius capetinga* is endemic to the Cerrado and an inhabitant of gallery forests. The Cerrado plateaus harbor the headwaters of major South American rivers; therefore, gallery forests form an extensive network through which many Amazonian and Atlantic Forest species penetrate deeply within Cerrado (Redford and Fonseca 1986; Oliveira-Filho and Ratter 1995; Silva 1996; Costa 2003). In general, gallery forests of the central and southern Cerrado have stronger affinities with the Atlantic Forest than with Amazonia, presumably because of their shared higher elevations and lower temperatures (Oliveira-Filho and Ratter 1995; Silva 1996). Gallery forests also provide routes for biotic exchange between Amazonian and Atlantic Forest during climatic fluctuations (Ledo and Colli 2017). Considering that an Atlantic Forest distribution is ancestral for *Enyalius* (Rodrigues et al. 2014), *E. capetinga* probably diverged from an Atlantic Forest ancestor that colonized Cerrado gallery forests and underwent geographical or ecological speciation.

The divergence between *E. capetinga* and its closest relative, *E. bilineatus*, is estimated to have occurred in the late Miocene at ~6.86 mya (confidence interval = 5.09–8.69; Rodrigues et al. 2014). Following a warm climate optimum in the middle Miocene, the late Miocene was characterized by global cooling and aridity driven by Andean orogeny, with pronounced effects in South America (Zachos et al. 2001, 2008; Armijo et al. 2015). This was accompanied by replacement of forests by open habitats in South America (Hynek et al. 2012; Le Roux 2012; Palazzesi and Barreda 2012; Pound et al. 2012; Nie et al. 2016). Gallery forests can exhibit similar dynamics to upland tropical forests during climate fluctuations, and their borders can retreat or advance over adjacent savannas (Silva et al. 2008). Therefore, under unfavorable conditions, gallery forests might shrink or even become fragmented, with profound effects on their environmental conditions caused by climate, soil, vegetation, and fire feedbacks (Hoffmann et al. 2002; Beckage et al. 2009; Staver and Levin 2012; MacDermott et al. 2017). We hypothesize that this resulted in the differentiation of *E. capetinga* from its ancestral clade through range fragmentation and/or a steepened ecological gradient between the Atlantic Forest and Cerrado gallery forests.

*Enyalius capetinga* has the smallest SVL of any species of *Enyalius*, and this could reflect a correlation between morphology and the use of more open vegetation or ground-level habitats relative to its congeners, as observed among Greater Antillean anoles (Losos 2009). Given the availability of a recent phylogenetic hypothesis (Rodrigues et al. 2014), future studies should explore the effects of habitat shifts on the evolution of morphological and ecological traits (e.g., behavioral, reproductive, and thermal ecology) among species of *Enyalius*.

The known populations of *Enyalius capetinga* are all under some level of threat. Even though the Distrito Federal populations occur inside protected areas, they are facing increased pressures including the complete isolation of these areas because of the expansion of urban areas, which leads to increasing levels of ecological disturbance by fires, pollution, local climate change, logging, and introduced species (UNESCO 2002; Françoso et al. 2015). Outside of protected areas (e.g., populations in Paracatu and Unaí), these conditions are exacerbated by the rapid conversion of natural Cerrado habitats into crops and pastureland (Jepson et al. 2010; Sano et al. 2010), and by recent changes in the Brazilian Forest Code that reduce the protection of gallery forests (Ledo and Colli 2016). The future seems bleak for *E. capetinga* and many other Cerrado endemics that depend on gallery forests; thus, the need to understand the biology and evolutionary history of these species cannot be understated, in order to provide improved taxonomic and ecological foundations for conservation.

**Acknowledgments.**—We thank A.S. Arruda Camara Cabral and N. Cazzaniga for discussion and references clarifying the derivation of the word "capetinga," and L.J. Ávila for help with scale nomenclature. We thank J. Lozier for providing office space during an internship at the University of Alabama. We thank the following collections and their curators for loaning

specimens: MZUSP (Museu de Zoologia da Universidade de São Paulo), MCP (Museu de Ciências e Tecnologia da Pontifícia Universidade Católica do Rio Grande do Sul), ZUEC (Museu de Zoologia da Universidade de Campinas), MNRJ (Museu Nacional da Universidade Federal do Rio de Janeiro), MPEG (Museu Paraense Emílio Goeldi), MZUFV (Museu de Zoologia João Moojen da Universidade Federal de Viçosa), and MCNR (Coleção de Herpetologia do Museu de Ciências Naturais da Pontifícia Universidade Católica de Minas Gerais). This research was supported by the following postdoctoral fellowships: Programa Nacional de Pós-Doutorado—CAPES (MFB), Partnerships for Enhanced Engagement in Research (PEER—USAID) (FMCBD), CNPq Ciência Sem Fronteiras Young Talent Fellow award (JCB), and a PROCAD award (HW). GRC thanks CAPES, CNPq, Fundação de Apoio à Pesquisa do Distrito Federal (FAPDF), and the USAID's PEER program under cooperative agreement AID-OAA-A-11-00012 for financial support.

## SUPPLEMENTAL MATERIAL

Supplemental material associated with this article can be found online at https://doi.org/10.1655/Herpetologica-D-17-00041.S1; https://doi.org/10.1655/Herpetologica-D-17-00041.S2; https://doi.org/10.1655/Herpetologica-D-17-00041.S3; https://doi.org/10.1655/Herpetologica-D-17-00041.S4; https://doi.org/10.1655/Herpetologica-D-17-00041.S5; https://doi.org/10.1655/Herpetologica-D-17-00041.S6; https://doi.org/10.1655/Herpetologica-D-17-00041.S7; https://doi.org/10.1655/Herpetologica-D-17-00041.S8; https://doi.org/10.1655/Herpetologica-D-17-00041.S9; https://doi.org/10.1655/Herpetologica-D-17-00041.S10.

## LITERATURE CITED

Aberer, A.J., K. Kobert, and A. Stamatakis. 2014. ExaBayes: Massively parallel Bayesian tree inference for the whole-genome era. Molecular Biology and Evolution 31:2553–2556.

Agnarsson, I., and M. Kuntner. 2007. Taxonomy in a changing world: Seeking solutions for a science in crisis. Systematic Biology 56:531–539.

Alvares, C.A., J.L. Stape, P.C. Sentelhas, J.L.D. Goncalves, and G. Sparovek. 2013. Köppen's climate classification map for Brazil. Meteorologische Zeitschrift 22:711–728.

Armijo, R., R. Lacassin, A. Coudurier-Curveur, and D. Carrizo. 2015. Coupled tectonic evolution of Andean orogeny and global climate. Earth-Science Reviews 143:1–35.

Bagley, J.C. 2017. justincbagley/GaussClust: GaussClust, Version 0.1.0 [Data Set]. Zenodo. Available via http://doi.org/10.5281/zenodo.231221. Archived by WebCite at http://www.webcitation.org/6rjTFt5SW on 5 July 2017.

Barreto-Lima, A.F. 2012. Distribuição, Nicho Potencial e Ecologia Morfológica do Gênero *Enyalius* (Squamata, Leiosauridae): Testes de Hipóteses para Lagartos de Florestas Continentais Brasileiras. Ph.D. dissertation, Universidade Federal do Rio Grande do Sul, Brazil.

Barreto-Lima, A.F., and B.M. Sousa. 2011. Feeding ecology and sexual dimorphism of *Enyalius perditus* in an Atlantic forest, Brazil. Herpetological Bulletin 118:1–9.

Beckage, B., W.J. Platt, and L.J. Gross. 2009. Vegetation, fire, and feedbacks: A disturbance-mediated model of savannas. American Naturalist 174:805–818.

Biecek, P., E. Szczurek, M. Vingron, and J. Tiuryn. 2012. The R package bgmm: Mixture modeling with uncertain knowledge. Journal of Statistical Software 47:1–31.

Bokermann, W.C.A. 1957. Atualização do itinerario da viagem do Principe de Wied ao Brasil (1815–1817). Arquivos de Zoologia (São Paulo) 10:209–251.

Boulenger, G.A. 1885. A list of reptiles and batrachians from the province Rio Grande do Sul, Brazil, sent to the Natural History Museum by Dr. H. von Ihering. The Annals and Magazine of Natural History 15:191–196.

Breiman, L. 2001. Random forests. Machine Learning 45:5–32.

Breiman, L., and P. Spector. 1992. Submodel selection and evaluation in regression. The X-random case. International Statistical Review 60:291–319.

Breitman, M.F., L.J. Avila, J.W. Sites, Jr., and M. Morando. 2012. How lizards survived blizzards: Phylogeography of the *Liolaemus lineomaculatus* group (Liolaemidae) reveals multiple breaks and refugia in southern Patagonia and their concordance with other codistributed taxa. Molecular Ecology 21:6068–6085.

Costa, H.C., and R.S. Bérnils. 2014. Répteis brasileiros: Lista de espécies 2015. Herpetologia Brasileira 4:75–93.

Costa, L.P. 2003. The historical bridge between the Amazon and the Atlantic Forest of Brazil: A study of molecular phylogeography with small mammals. Journal of Biogeography 30:71–86.

Cutler, D.R., T.C. Edwards, K.H. Beard, A. Cutler, and K.T. Hess. 2007. Random forests for classification in ecology. Ecology 88:2783–2792.

Dayrat, B. 2005. Towards integrative taxonomy. Biological Journal of the Linnean Society 85:407–415.

de Queiroz, K. 2007. Species concepts and species delimitation. Systematic Biology 56:879–886.

Deng, H. 2013. Guided random forest in the RRF package. arXiv 1306.0237v1:1–2.

Domingos, F.M.C.B., R.J. Bosque, J. Cassimiro, G.R. Colli, M.T. Rodrigues, M.G. Santos, and L.B. Beheregaray. 2014. Out of the deep: Cryptic speciation in a Neotropical gecko (Squamata, Phyllodactylidae) revealed by species delimitation methods. Molecular Phylogenetics and Evolution 80:113–124.

Drew, L.W. 2011. Are we losing the science of taxonomy? BioScience 61:942–946.

Duméril, A.M.C., and G. Bibron. 1837. Erpétologie Générale ou Histoire Naturelle Complète des Reptiles. Tome Quatrième. Librairie Encyclopédique de Roret, France.

Etheridge, R. 1969. A review of the iguanid lizard genus *Enyalius*. Bulletin of the British Museum (Natural History) 18:231–260.

Felsenstein, J., and H. Kishino. 1993. Is there something wrong with the bootstrap on phylogenies? A reply to Hillis and Bull. Systematic Biology 42:193–200.

Françoso, R.D., R. Brandão, C.C. Nogueira, Y.B. Salmona, R.B. Machado, and G.R. Colli. 2015. Habitat loss and the effectiveness of protected areas in the Cerrado Biodiversity Hotspot. Natureza & Conservação 13:35–40.

Frost, D.R., R. Etheridge, D. Janies, and T.A. Titus. 2001. Total evidence, sequence alignment, evolution of polychrotid lizards, and a reclassification of the Iguania (Squamata: Iguania). American Museum Novitates 3343:1–38.

Hillis, D.M., and J.J. Bull. 1993. An empirical test of bootstrapping as a method for assessing confidence in phylogenetic analysis. Systematic Biology 42:182–192.

Hoffmann, W.A., W. Schroeder, and R.B. Jackson. 2002. Positive feedbacks of fire, climate, and vegetation and the conversion of tropical savanna. Geophysical Research Letters 29:4.

Houle, D. 1992. Comparing evolvability and variability of quantitative traits. Genetics 130:195–204.

Huelsenbeck, J.P., and F. Ronquist. 2001. MRBAYES: Bayesian inference of phylogenetic trees. Bioinformatics 17:754–755.

Hynek, S.A., B.H. Passey, J.L. Prado, F.H. Brown, T.E. Cerling, and J. Quade. 2012. Small mammal carbon isotope ecology across the Miocene–Pliocene boundary, northwestern Argentina. Earth and Planetary Science Letters 321:177–188.

Jackson, J.F. 1978. Differentiation in the genera *Enyalius* and *Strobilurus* (Iguanidae): Implications for Pleistocene climatic changes in eastern Brazil. Arquivos de Zoologia (São Paulo) 30:1–79.

Jepson, W., C. Brannstrom, and A. Filippi. 2010. Access regimes and regional land change in the Brazilian Cerrado, 1972–2002. Annals of the Association of American Geographers 100:87–111.

Kearse, M., R. Moir, A. Wilson . . . A. Drummond. 2012. Geneious Basic: An integrated and extendable desktop software platform for the organization and analysis of sequence data. Bioinformatics 28:1647–1649.

Kohavi, R. 1995. A study of cross-validation and bootstrap for accuracy estimation and model selection. Pp. 1137–1143 in Proceedings of the 14th International Joint Conference on Artificial Intelligence, Volume 2 (IJCAI95, ed.). Morgan Kaufmann Publishers, Inc., Canada.

Lanfear, R., B. Calcott, S.Y.W. Ho, and S. Guindon. 2012. PartitionFinder: Combined selection of partitioning schemes and substitution models for phylogenetic analyses. Molecular Biology and Evolution 29:1695–1701.

Lanfear, R., B. Calcott, D. Kainer, C. Mayer, and A. Stamatakis. 2014. Selecting optimal partitioning schemes for phylogenomic datasets. BMC Evolutionary Biology 14:14.

Lanfear, R., P.B. Frandsen, A.M. Wright, T. Senfeld, and B. Calcott. 2017. PartitionFinder 2: New methods for selecting partitioned models of evolution for molecular and morphological phylogenetic analyses. Molecular Biology and Evolution 34:772–773.

Le Roux, J.P. 2012. A review of Tertiary climate changes in southern South

America and the Antarctic Peninsula. Part 2: Continental conditions. Sedimentary Geology 247:21–38.
Ledo, R.M.D., and G.R. Colli. 2016. Silent death: The new Brazilian Forest Code does not protect lizard assemblages in Cerrado riparian forests. South American Journal of Herpetology 11:98–109.
Ledo, R.M.D., and G.R. Colli. 2017. The historical connections between the Amazon and the Atlantic Forest revisited. Journal of Biogeography 44:2551–2563.
Lesson, R.P. 1830. Description de quelques reptiles nouveaux ou peu connus. Pp. 1–65 in Voyage Autour du Monde, Exécuté par Ordre du Roi, sur la Corvette de Sa Majesté, La Coquille, Pendant les Années 1822, 1823, 1824 et 1825. Zoologie, Tome Second. (M.L.I. Duperrey, ed.). Arthur Bertrand, France.
Losos, J.B. 2009. Lizards in an Evolutionary Tree: Ecology and Adaptive Radiation of Anoles. University of California Press, USA.
MacDermott, H.J., R.J. Fensham, Q. Hua, and D. Bowman. 2017. Vegetation, fire, and soil feedbacks of dynamic boundaries between rainforest, savanna and grassland. Austral Ecology 42:154–164.
Maia-Carneiro, T., T. Motta-Tavares, D. Vrcibradic, M.C. Kiefer, T.A. Dorigo, C.F.D. Rocha, and M. Van Sluys. 2016. Feeding habits of *Enyalius perditus* (Squamata: Leiosauridae) in an Atlantic Forest remnant in southeastern Brazil. Phyllomedusa 15:21–27.
Mingers, J. 1989. An empirical comparison of selection measures for decision-tree induction. Machine Learning 3:319–342.
Mirarab, S., N. Nguyen, S. Guo, L.S. Wang, J. Kim, and T. Warnow. 2015. PASTA: Ultra-large multiple sequence alignment for nucleotide and amino-acid sequences. Journal of Computational Biology 22:377–386.
Moraes, P.L.R. 2009. The Brazilian herbarium of Maximilian, Prince of Wied. Neodiversity 4:16–51.
Moraes, P.L.R. 2011. Notes and lectotypification of names based on Brazilian collections of Prince Maximilian of Wied. Kew Bulletin 66:493–503.
Murphy, J.C., M.J. Jowers, R.M. Lehtinen, S.P. Charles, G.R. Colli, A.K. Peres, C.R. Hendry, and R.A. Pyron. 2016. Cryptic, sympatric diversity in tegu lizards of the *Tupinambis teguixin* group (Squamata, Sauria, Teiidae) and the description of three new species. PloS One 11:e0158542. DOI: https://doi.org/10.1371/journal.pone.0158542.
Nagy, Z.T., G. Sonet, F. Glaw, and M. Vences. 2012. First large-scale DNA barcoding assessment of reptiles in the biodiversity hotspot of Madagascar, based on newly designed COI primers. PloS One 7:e34506. DOI: https://doi.org/10.1371/journal.pone.0034506.
Nie, Z.L., V.A. Funk, Y. Meng, T. Deng, H. Sun, and J. Wen. 2016. Recent assembly of the global herbaceous flora: Evidence from the paper daisies (Asteraceae: Gnaphalieae). New Phytologist 209:1795–1806.
Nogueira, C., G.R. Colli, and M. Martins. 2009. Local richness and distribution of the lizard fauna in natural habitat mosaics of the Brazilian Cerrado. Austral Ecology 34:83–96.
Oliveira-Filho, A.T., and J.A. Ratter. 1995. A study of the origin of central Brazilian forests by the analysis of plant species distribution patterns. Edinburgh Journal of Botany 52:141–194.
Oliveira-Filho, A.T., and J.A. Ratter. 2002. Vegetation physiognomies and woody flora of the Cerrado biome. Pp. 91–120 in The Cerrados of Brazil: Ecology and Natural History of a Neotropical Savanna (P.S. Oliveira and R.J. Marquis, eds.). Columbia University Press, USA.
Padial, J.M., A. Miralles, I. De la Riva, and M. Vences. 2010. The integrative future of taxonomy. Frontiers in Zoology 7:16.
Palazzesi, L., and V. Barreda. 2012. Fossil pollen records reveal a late rise of open-habitat ecosystems in Patagonia. Nature Communications 3:1294.
Pante, E., C. Schoelinck, and N. Puillandre. 2015. From integrative taxonomy to species description: One step beyond. Systematic Biology 64:152–160.
Pound, M.J., A.M. Haywood, U. Salzmann, and J.B. Riding. 2012. Global vegetation dynamics and latitudinal temperature gradients during the mid to late Miocene (15.97–5.33 Ma). Earth-Science Reviews 112:1–22.
Quinn, G.P., and M.J. Keough. 2002. Experimental Design and Data Analysis for Biologists. Cambridge University Press, UK.
R Core Team. 2017. R: A Language and Environment for Statistical Computing, Version v3.3.1. Available at https://cran.r-project.org. R Foundation for Statistical Computing, Austria.
Ramos, A.M., L.A.R. dos Santos, and L.T.G. Fortes. 2009. Normais Climatológicas do Brasil 1961–1990. INMET, Brazil.
Ratnasingham, S., and P.D.N. Hebert. 2007. BOLD: The Barcode of Life Data System. Molecular Ecology Notes 7:355–364.
Rautenberg, R., and R.R. Laps. 2010. Natural history of the lizard *Enyalius iheringii* (Squamata, Leiosauridae) in southern Brazilian Atlantic forest. Iheringia Série Zoologia 100:287–290.
Redford, K.H., and G.A.B. Fonseca. 1986. The role of gallery forests in the zoogeography of the Cerrado non-volant mammalian fauna. Biotropica 18:126–135.
Rodrigues, M.T., M.A. Freitas, T.F.S. Silva, and C.E.V. Bertolotto. 2006. A new species of lizard genus *Enyalius* (Squamata, Leiosauridae) from the highlands of Chapada Diamantina, state of Bahia, Brazil, with a key to species. Phyllomedusa 5:11–24.
Rodrigues, M.T., C.E.V. Bertolotto, R.C. Amaro, Y. Yonenaga-Yassuda, E.M.X. Freire, and K.C.M. Pellegrino. 2014. Molecular phylogeny, species limits, and biogeography of the Brazilian endemic lizard genus *Enyalius* (Squamata: Leiosauridae): An example of the historical relationship between Atlantic Forests and Amazonia. Molecular Phylogenetics and Evolution 81:137–146.
Sangster, G., and J.A. Luksenburg. 2015. Declining rates of species described per taxonomist: Slowdown of progress or a side-effect of improved quality in taxonomy? Systematic Biology 64:144–151.
Sano, E.E., R. Rosa, J.L.S. Brito, and L.G. Ferreira. 2010. Land cover mapping of the tropical savanna region in Brazil. Environmental Monitoring and Assessment 166:113–124.
Schinz, H.R. 1822. Das Thierreich eingetheilt nach dem Bau der Thiere: als Grundlage ihrer Naturgeschichte und der vergleichenden Anatomie. Zweiter Band. Reptilien, Fische, Weichthiere, Ringelwürmer. J.G. Cotta'schen Buchhandlung, Germany.
Silva, J.M.C. 1996. Distribution of Amazonian and Atlantic birds in gallery forests of the Cerrado region, South America. Ornitologia Neotropical 7:1–18.
Silva, L.C.R., L. Sternberg, M. Haridasan, W.A. Hoffmann, F. Miralles-Wilhelm, and A.C. Franco. 2008. Expansion of gallery forests into central Brazilian savannas. Global Change Biology 14:2108–2118.
Smith, H.M. 1946. Handbook of Lizards: Lizards of the United States and of Canada. Comstock Publishing Company, USA.
Stamatakis, A. 2014. RAxML version 8: A tool for phylogenetic analysis and post-analysis of large phylogenies. Bioinformatics 30:1312–1313.
Staver, A.C., and S.A. Levin. 2012. Integrating theoretical climate and fire effects on savanna and forest systems. American Naturalist 180:211–224.
Sturaro, M.J., and V.X. da Silva. 2010. Natural history of the lizard *Enyalius perditus* (Squamata: Leiosauridae) from an Atlantic forest remnant in southeastern Brazil. Journal of Natural History 44:1225–1238.
UNESCO (United Nations Educational, Scientific and Cultural Organization). 2002. Vegetação do Distrito Federal: Tempo e Espaço. UNESCO, Brazil.
van Buuren, S., and K. Groothuis-Oudshoorn. 2011. mice: Multivariate imputation by chained equations in R. Journal of Statistical Software 45:1–67.
Vargas, S.M., M.d.O. Santos, I.A. Novelli, ... B.M. de Sousa. 2015. Genetic diversity and structure of two species of *Enyalius* (Squamata: Leiosauridae) from Neotropical biodiversity hotspots. Phyllomedusa 14:99–111.
Vitt, L.J., T.C.S. Avila-Pires, and P.A. Zani. 1996. Observations on the ecology of the rare Amazonian lizard, *Enyalius leechii* (Polychrotidae). Herpetological Natural History 4:77–82.
Wagler, J. 1830. Natürliches System der Amphibien, mit vorangehender Classification der Säugethiere und Vögel. Ein Beitrag zur vergleichenden Zoologie. J.G. Cotta'schen Buchhandlung, Germany.
Weston, J., C. Leslie, E. Ie, D.Y. Zhou, A. Elisseeff, and W.S. Noble. 2005. Semi-supervised protein classification using cluster kernels. Bioinformatics 21:3241–3247.
Wheeler, Q.D. 2004. Taxonomic triage and the poverty of phylogeny. Philosophical Transactions of the Royal Society of London Series B—Biological Sciences 359:571–583.
Wied-Neuwied, M. 1821. Reise nach Brasilien in den Jahren 1815 bis 1817. Zweiter Band. Heinrich Ludwig Brönner, Germany.
Wilson, E.O. 1985. The biological diversity crisis. BioScience 35:700–706.
Yang, Z. 2015. The BPP program for species tree estimation and species delimitation. Current Zoology 61:854–865.
Yang, Z., and B. Rannala. 2010. Bayesian species delimitation using multilocus sequence data. Proceedings of the National Academy of Sciences 107:9264–9269.
Yang, Z., and B. Rannala. 2014. Unguided species delimitation using DNA sequence data from multiple loci. Molecular Biology and Evolution 31:3125–3135.
Zachos, J., M. Pagani, L. Sloan, E. Thomas, and K. Billups. 2001. Trends, rhythms, and aberrations in global climate 65 Ma to present. Science 292:686–693.
Zachos, J.C., G.R. Dickens, and R.E. Zeebe. 2008. An early Cenozoic

perspective on greenhouse warming and carbon-cycle dynamics. Nature 451:279–283.

Zatz, M.G. 2002. O Polimorfismo Cromático e sua Manutenção em *Enyalius* sp. (Squamata: Leiosauridae) no Cerrado do Brasil Central. Master's thesis, Universidade de Brasília, Brazil.

**Accepted on** 8 August 2018
**Associate Editor:** Matthew Fujita

## APPENDIX

List of the morphological characters used in comparisons among species of *Enyalius*, including their acronyms in parentheses. Where necessary, we list clarifications and different states of the character in question. Asterisks indicate characters and states that were monomorphic for our *Enyalius* samples.

### Qualitative Characters

1. Canthus rostralis (CRo), shape: (0) incomplete, (1) complete.
2. Nasal (N), shape: (0) asymmetric, *(1) symmetric.
3. Supraoculars (SpO), form: *(0) smooth, (1) conic or pyramidal, (2) keeled.
4. Auriculars (A), pattern: (0) homogeneous, (1) heterogeneous.
5. Intercanthals (IntC), form of scales between nostrils and anterior region of the eyes: *(0) smooth, (1) pyramidal, (2) keeled.
6. Canthal ridge scales (CRiS), form: *(0) smooth, (1) not smooth.
7. Supracarpals (SpC), form: (0) smooth, (1) keeled.
8. Infracarpals (InC), form: (0) smooth, (1) keeled.
9. Infrabrachials (InB), form: (0) granular, (1) keeled, (2) mixed.
10. Suprafemorals (SpF), form: *(0) smooth, (1) keeled, (2) predominantly keeled
11. Infrafemorals (InF), form: (0) smooth, (1) keeled.
12. Infratibials (InT), form: *(0) smooth, (1) keeled.
13. Dorsal crest scales (DCS), form: (0) pyramidal, (1) spinelike shape, (2) keeled, (3) conic.
14. Tail crest scales (TCS), from the base until 1/3 of tail length: *(0) absent, (1) present.
15. Paravertebral scales (PVS), form: (0) pyramidal keeled, (1) elongated keeled, (2) mixed keeled, (3) conic not keeled, (4) elongated not keeled.
16. Dorsal scales (DS), form of dorsal scales excluding crest scales form: (0) mostly smooth, (1) mostly granular, (2) mostly keeled.
17. Lateral scales (LS), form: (0) granular, (1) conic or pyramidal, (2) keeled.
18. Ventral scales (VnS), form: (0) smooth, (1) keeled.
19. Nasal/postrostral contact (NPRC): (0) absent, (1) present.
20. Subocular (SbO), size: (0) enlarged, (1) small.
21. Gular fold (GF), defined by smaller scales inside fold: (0) absent, (1) present.
22. External gular fold scales (EGFS), form: (0) smooth, (1) keeled.
23. Dorsal head scales (DHS), form: (0) smooth, (1) conic, (2) keeled.
24. Mental (M), form: (0) flat, (1) triangular.
25. Supratarsal keels (SpTK), type of keels: *(0) unicarinated, (1) multicarinated.
26. Fourth toe lamellae (4TL), form: (0) smooth, (1) keeled.
27. Fourth finger lamellae (4FL), form: (0) smooth, (1) keeled.
28. Dorsal crest (DC): (0) absent, (1) present.

### Meristic Characters

29. Paravertebral scales (nPVS), number of scales between posterior edge of forelimb and anterior edge of hindlimb insertions.
30. Midbody scales (nMS), one half the number of scales around the midbody.
31. Vertebral scales (nVrS), number of scales between interparietal scale and posterior edge of hindlimb insertions.
32. Ventral scales (nVnS), number of scales between posterior edge of forelimb and anterior edge of hindlimb insertions.
33. Infralabials (nInL), number.
34. Postmentals (nPM), number.
35. Contact postmentals (ncPM), number of scales in contact with postmental scales.
36. Gular scales (nGS), number of scales between mental scale and gular fold.
37. Canthus rostralis (nCRo), number of scales located in the canthus rostralis.
38. Between nasal and supralabials (nbNSpL), minimum number of scales between nasal and supralabial scales.
39. Loreal series (nLS), minimum count.
40. Contact interparietal (ncIp), number of scales in contact with interparietal.
41. Between circumorbital arcs (nbCoA), minimum number of scales.
42. Supralabials (nSpL), number.
43. Postrostrals (nPR), number.
44. Suboculars (nSbO), number.
45. Supraciliaries (nSpC), number.
46. Between subocular and supralabials (nbSbOSpL), number of scales.
47. Fourth toe lamellae (n4TL), number.
48. Fourth finger lamellae (n4FL), number.
49. Sulcated fourth finger lamellae (n4FL1), number.
50. Dorsolateral tibials (nDlT), number.
51. Around the tail (nArT), number of scales around the tail at the first ring after the cloaca.
52. Along the tail (nAlT), number of scales between cloaca and tip of the tail.

### Morphometric Characters

53. Tail length (TL), length between cloacae and tip of the tail.
54. Snout–vent length (SVL), ventral length between mental and cloacae.